Cell

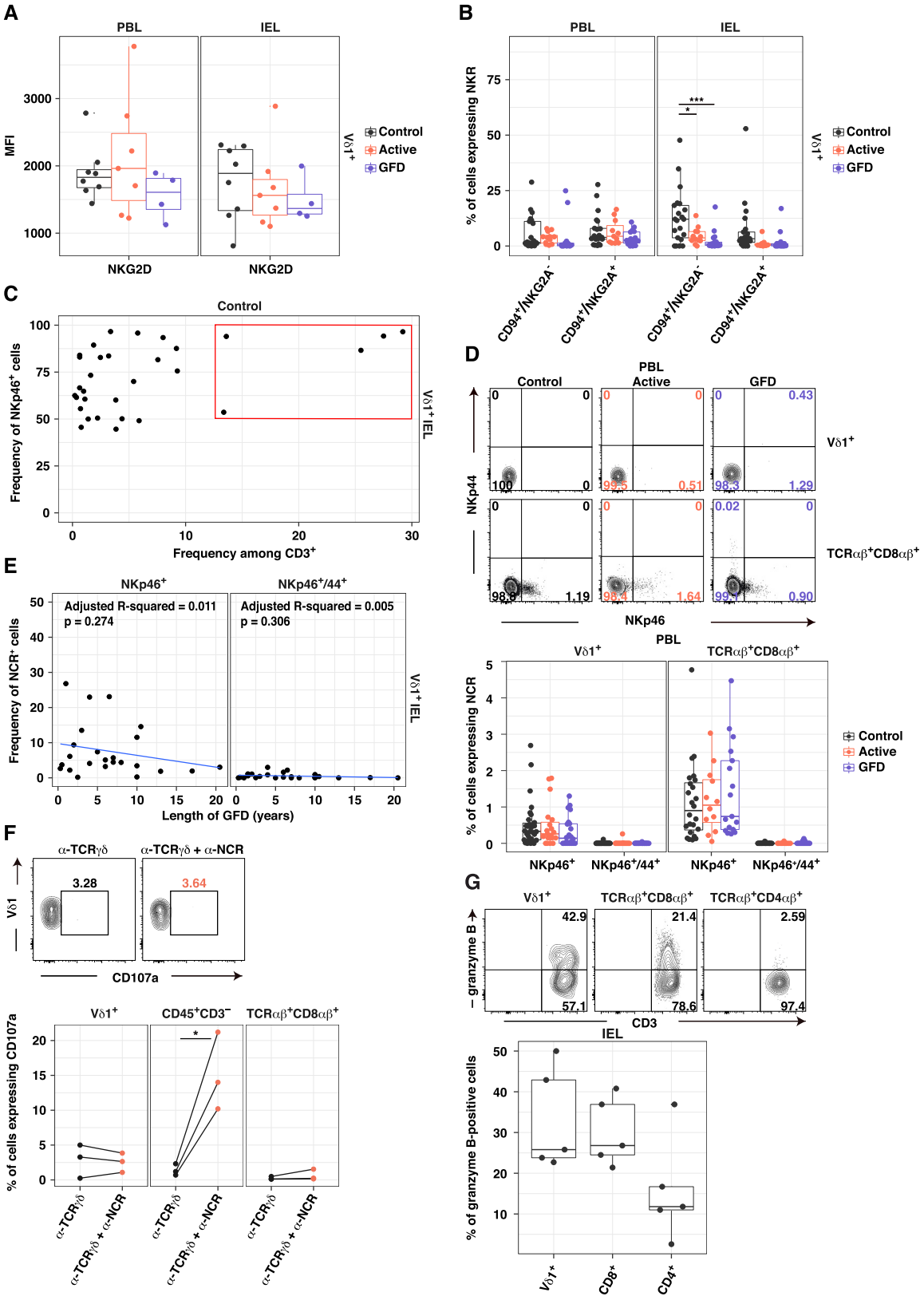

(legend on next page)

Figure S1. Innate-like Vδ1$^+$ IELs Are Lost in CeD, Related to Figure 2

(A) Expression of NKG2D on Vδ1$^+$ PBLs and IELs. Boxplots display first and third quartiles. (B) Expression of CD94 and NKG2A on Vδ1$^+$ PBLs and IELs. Boxplots display first and third quartiles. CD94$^+$/NKG2A$^-$, activating; CD94$^+$/NKG2A$^+$, inhibitory. *$p < 0.05$, ***$p < 0.001$. One-way ANOVA with Tukey's test for multiple comparisons. (C) Frequency of Vδ1$^+$ IELs expressing NKp46 among total CD3$^+$ lymphocytes. The red box depicts individuals with Vδ1$^+$ IEL expansions of similar magnitude to those found in patients with CeD. (D) Expression of NKp46 and NKp44 on PBLs. Bottom: boxplots display first and third quartiles. (E) Frequency of Vδ1$^+$ IELs expressing NKp46 or NKp46/NKp44 versus the duration of treatment with a GFD. (F) Expression of CD107a on Vδ1$^+$ IELs after stimulation with plate-bound αTCRγδ ± αNKp46 and αNKp44. *$p < 0.05$. Paired t test. (G) Expression of granzyme B among subsets of IELs. Bottom: boxplot displays first and third quartiles.

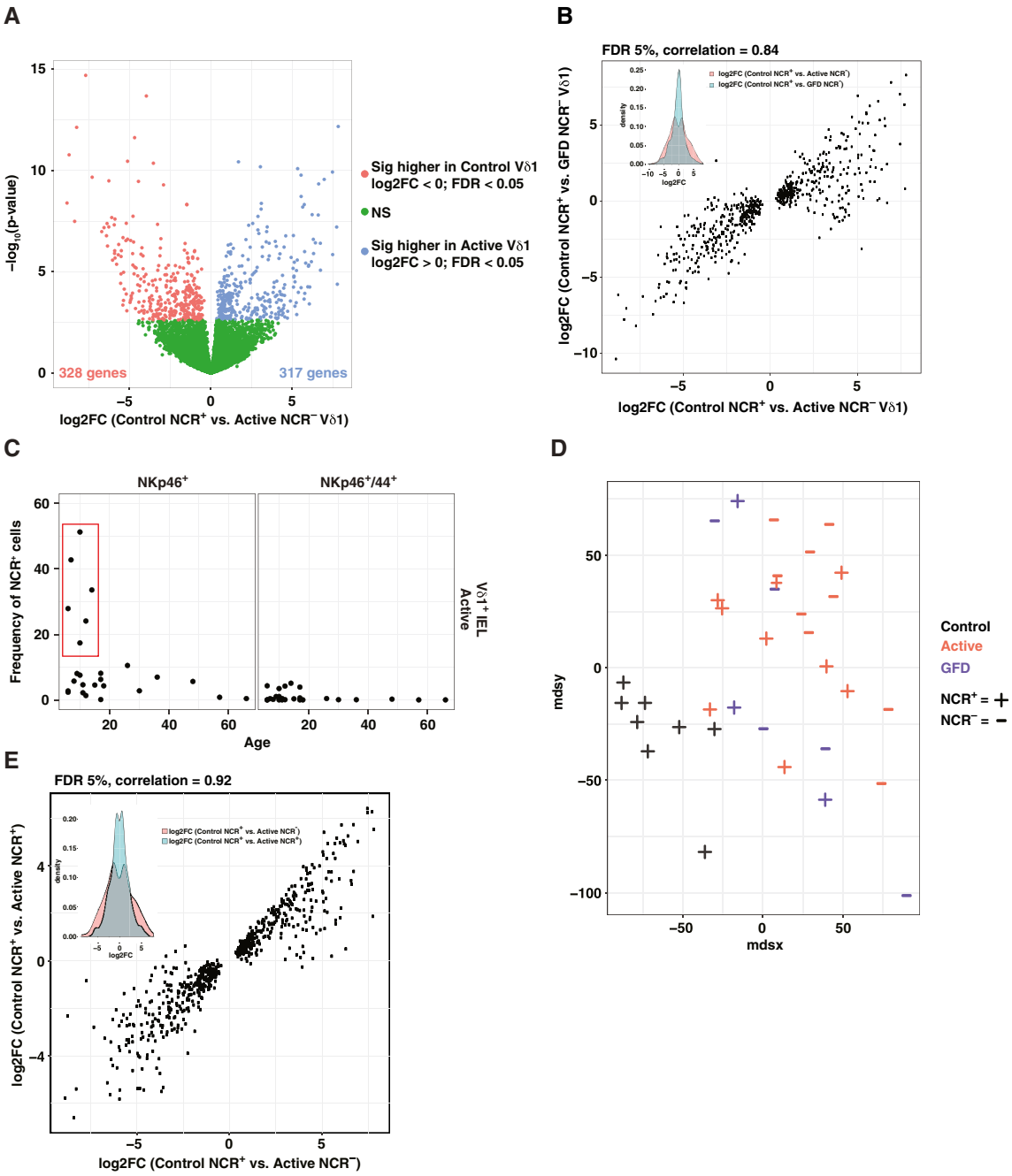

Figure S2. The Transcriptional Program of Vδ1$^+$ IELs Is Permanently Altered in CeD, Related to Figure 4

(A) Differentially expressed genes (DEGs) between NCR$^+$ Vδ1$^+$ IELs from healthy controls and NCR$^-$ Vδ1$^+$ IELs from patients with active CeD. DEGs highlighted in blue were more highly expressed in NCR$^-$ Vδ1$^+$ IELs from patients with active CeD (FDR < 5%), and DEGs highlighted in red were more highly expressed in NCR$^+$ Vδ1$^+$ IELs from healthy controls (FDR < 5%). (B) DEGs shown in (A) were used to correlate the magnitude of gene expression differences between NCR$^+$ Vδ1$^+$ IELs from healthy controls and NCR$^-$ Vδ1$^+$ IELs from patients with active CeD (x axis) versus the magnitude of gene expression differences between NCR$^+$ Vδ1$^+$ IELs from healthy controls and NCR$^-$ Vδ1$^+$ IELs from patients with GFD-treated CeD (y axis). Genes with $\log_2$FC values > 0 were more highly expressed in NCR$^-$ Vδ1$^+$ IELs from patients with active or GFD-treated CeD relative to NCR$^+$ Vδ1$^+$ IELs from healthy controls, and genes with $\log_2$FC values < 0 were more highly expressed in NCR$^+$ Vδ1$^+$ IELs from healthy controls relative to NCR$^-$ Vδ1$^+$ IELs from patients with active or GFD-treated CeD. Top left: $\log_2$FC distribution for all genes in the dot plot summarized as a histogram for each comparison. Pearson correlation. (C) Frequency of Vδ1$^+$ IELs expressing NKp46 or NKp46/NKp44 versus age for patients with active CeD. The red box depicts individuals < 16 years old with high frequencies of NKp46$^+$ Vδ1$^+$ IELs. (D) Multidimensional scaling plot showing gene expression profile similarity among NCR$^+$ Vδ1$^+$ IELs from healthy controls, NCR$^+$ Vδ1$^+$ IELs from patients with active CeD, NCR$^-$ Vδ1$^+$ IELs from patients with active CeD, NCR$^+$ Vδ1$^+$ IELs from patients with GFD-treated CeD, and NCR$^-$ Vδ1$^+$ IELs from patients with GFD-treated CeD. (E) DEGs shown in (A) were used to correlate the magnitude of gene expression differences between NCR$^+$ Vδ1$^+$ IELs from healthy controls and NCR$^-$ Vδ1$^+$ IELs from patients with active CeD (x axis)

(legend continued on next page)

versus the magnitude of gene expression differences between NCR$^+$ Vδ1$^+$ IELs from healthy controls and NCR$^+$ Vδ1$^+$ IELs from patients with active CeD (y axis). Genes with $\log_2$FC values > 0 were more highly expressed in NCR$^+$ and NCR$^-$ Vδ1$^+$ IELs from patients with active CeD relative to NCR$^+$ Vδ1$^+$ IELs from healthy controls, and genes with $\log_2$FC values < 0 were more highly expressed in NCR$^+$ Vδ1$^+$ IELs from healthy controls relative to NCR$^+$ and NCR$^-$ Vδ1$^+$ IELs from patients with active CeD. Top left: $\log_2$FC distribution for all genes in the dot plot summarized as a histogram for each comparison. Pearson correlation.

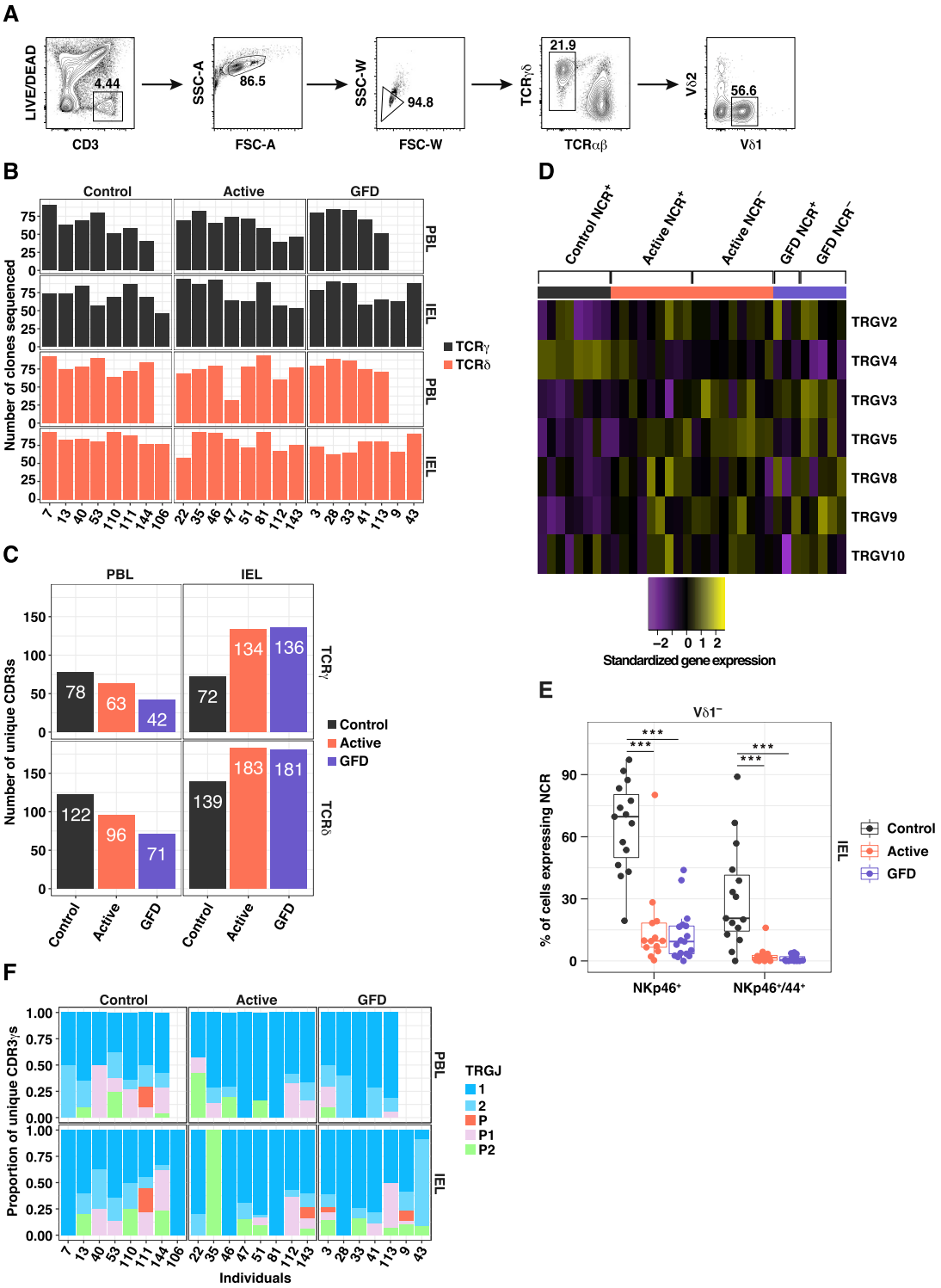

Figure S3. The *TRGV4* Gene-Associated "Gut Signature" Is Lost in CeD, Related to Figure 5

(A) Gating strategy: live CD3$^+$ TCRγδ$^+$ Vδ1$^+$ lymphocytes were flow-sorted for molecular analysis of expressed TCRs. (B) Number of clones per individual/tissue yielding productive sequences for TCRγ and TCRδ. (C) Number of unique CDR3 sequences per group/tissue for TCRγ and TCRδ. (D) Expression of *TRGV* genes in NCR$^+$ Vδ1$^+$ IELs from healthy controls (n = 8), NCR$^+$ Vδ1$^+$ IELs from patients with active CeD (n = 9), NCR$^-$ Vδ1$^+$ IELs from patients with active CeD (n = 9), NCR$^+$

(legend continued on next page)

Vδ1$^+$ IELs from patients with GFD-treated CeD (n = 3), and NCR$^-$ Vδ1$^+$ IELs from patients with GFD-treated CeD (n = 5). Germline transcripts were extracted from the RNA-seq dataset. Expression values were standardized (mean centered) on a per gene basis. (E) Frequency of Vδ1$^-$ IELs expressing NKp46 or NKp46/NKp44. Boxplot displays first and third quartiles. ***$p < 0.001$. One-way ANOVA with Tukey's test for multiple comparisons. (F) Proportion of unique CDR3γ sequences using a particular *TRGJ* gene summarized by individual.

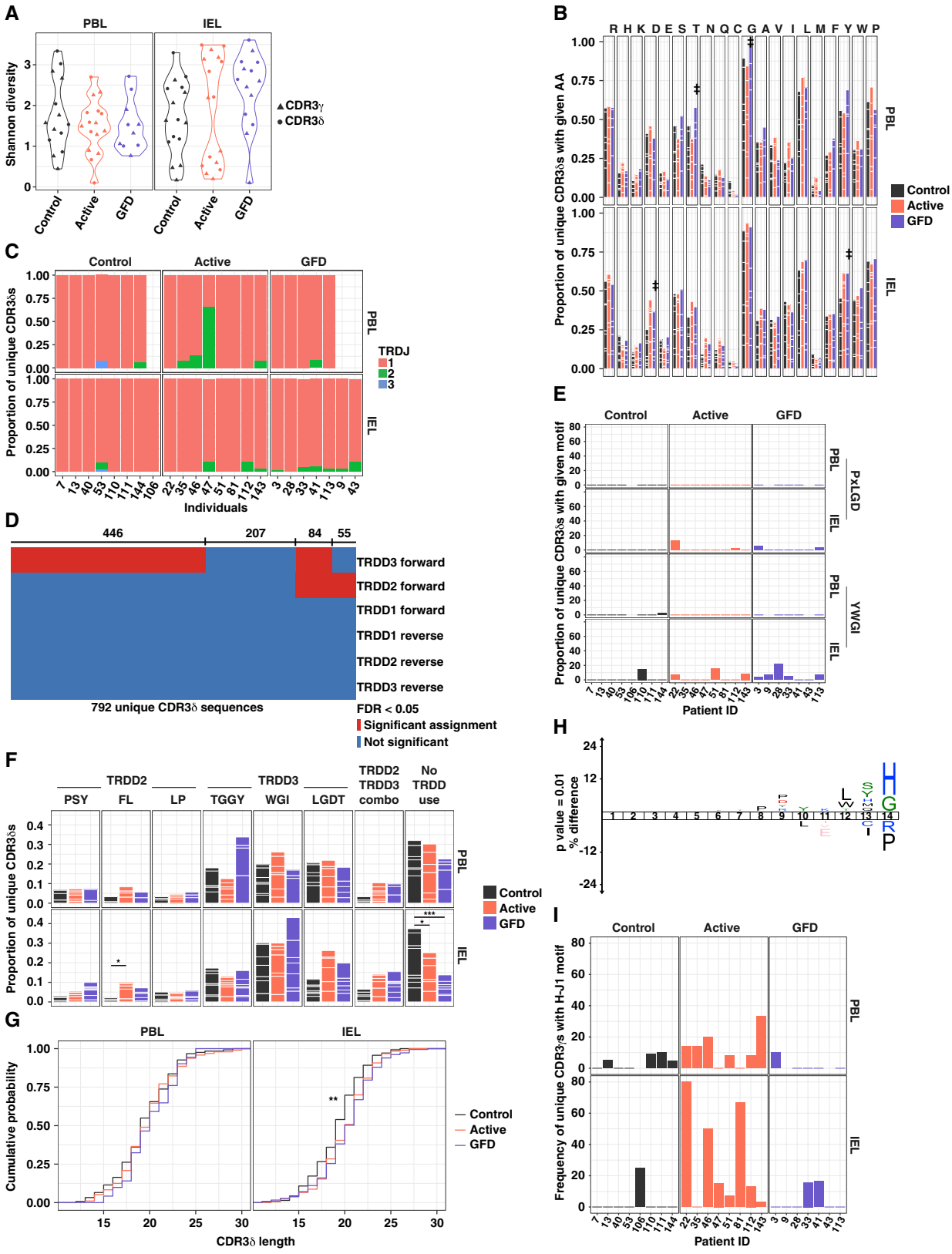

(legend on next page)

Figure S4. Vδ1$^+$ IELs Express TCRs with Longer CDR3δ Loops in CeD, Related to Figure 6

(A) Shannon diversity indices summarized in violin plots for CDR3γ and CDR3δ sequences. (B) Proportion of unique CDR3δ sequences using a particular amino acid (AA). White lines demarcate individual contributions. Healthy controls: PBLs, n = 7; IELs, n = 8. Patients with active CeD: PBLs, n = 8; IELs, n = 8. Patients with GFD-treated CeD: PBLs, n = 5; IELs, n = 7. ‡ denotes amino acids with significant differences between two groups. Firth's penalized logistic regression and beta regression. See Table S5C. (C) Proportion of unique CDR3δ sequences using a particular *TRDJ* gene summarized by individual. (D) Statistical assignment of *TRDD* gene use for each unique CDR3δ sequence. Each candidate forward and reverse *TRDD* gene sequence (rows) was tested for a significant substring match to each unique CDR3δ sequence (columns). Significant *TRDD* gene assignments (FDR < 0.05) are shown in red; non-significant *TRDD* gene assignments (FDR > 0.05) are shown in blue. (E) Frequency of unique CDR3δ sequences incorporating a particular motif summarized by individual. (F) Proportion of unique CDR3δ sequences using a particular feature. Healthy controls: PBLs, n = 7; IELs, n = 8. Patients with active CeD: PBLs, n = 8; IELs, n = 8. Patients with GFD-treated CeD: PBLs, n = 5; IELs, n = 7. *p < 0.05, ***p < 0.001. Firth's penalized logistic regression and beta regression. See Table S5D. (G) Cumulative distribution for CDR3δ length across groups. **p < 0.01. Kolmogorov-Smirnov test. (H) Unique CDR3γ sequences among Vδ1$^+$ IELs from patients with active CeD visualized using iceLogo for enrichment of non-germline-encoded amino acids relative to unique CDR3γ sequences among Vδ1$^+$ IELs from healthy controls and patients with GFD-treated CeD. Position 14 is closest to the *TRGJ* gene-encoded segment. (I) Frequency of unique CDR3γ sequences with an H-J1 motif summarized by individual.

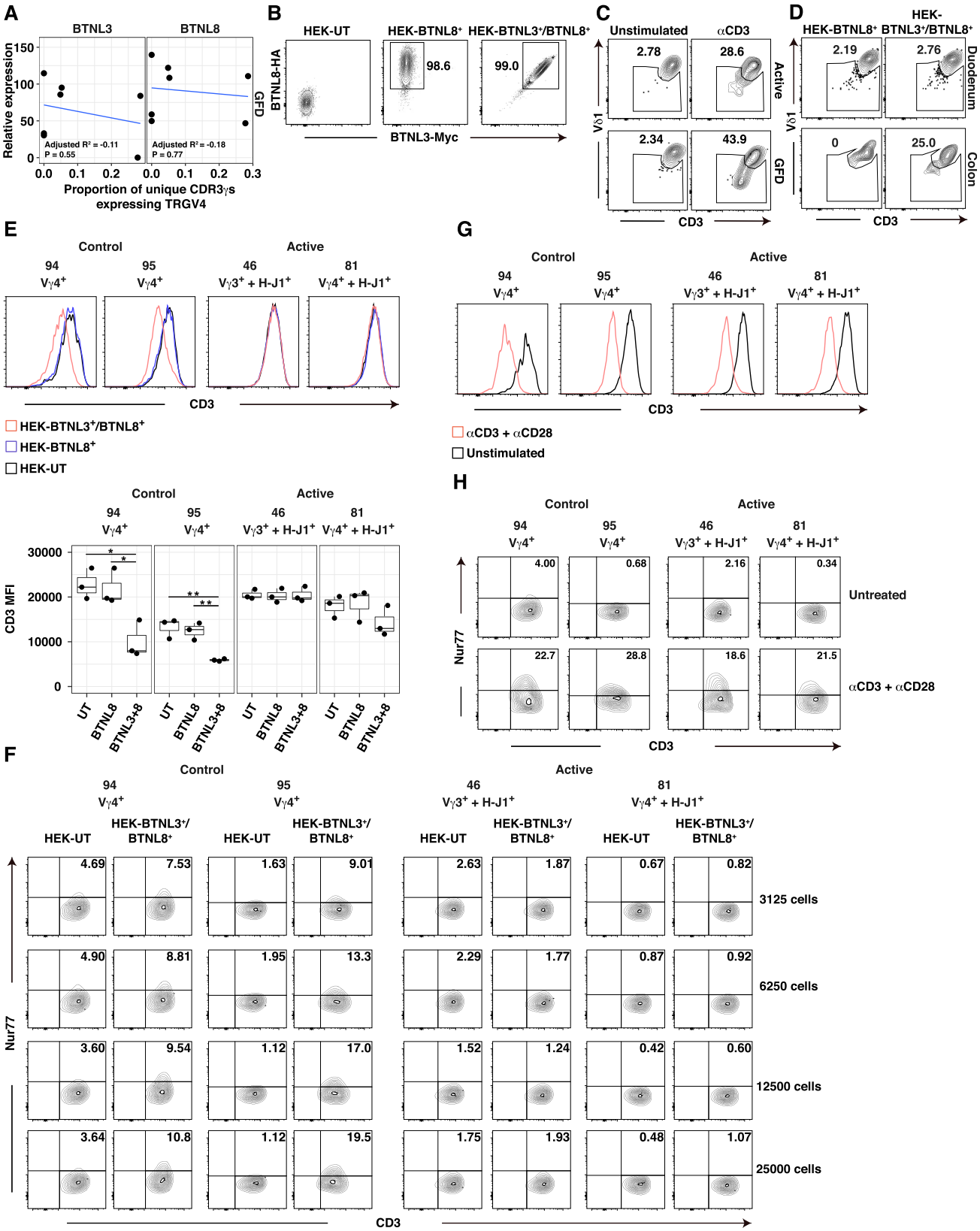

(legend on next page)

Figure S5. BTNL3/8-Reactive Vδ1$^+$ IELs Are Lost in CeD, Related to Figure 7

(A) Proportion of unique CDR3γ sequences using the *TRGV4* gene versus relative expression of *BTNL3* and *BTNL8* for patients with GFD-treated CeD. Linear regression. (B) Expression of BTNL3 (myc$^+$) and BTNL8 (HA$^+$) on untransduced (UT) HEK293T cells (left), HEK293T cells transduced with BTNL8-HA (middle), and HEK293T cells transduced with BTNL3-myc and BTNL8-HA (right). (C) Downregulation of CD3 and Vδ1 on the surface of IELs pre-gated for Vδ1 expression after stimulation for 2 hr with 1.5 μg/mL of plate-bound purified αCD3. (D) Downregulation of CD3 and Vδ1 on the surface of IELs pre-gated for Vδ1 expression after overnight incubation with HEK293T-BTNL8$^+$ or HEK293T-BTNL3/8$^+$ cells. (E) SKW3 cell lines stably expressing clonal TCRs were cultured overnight with HEK293T-UT (black), HEK293T-BTNL8$^+$ (blue), or HEK293T-BTNL3/8$^+$ cells (red). Top: representative histogram overlays displaying surface expression of CD3 on SKW3 cells. Bottom: boxplots show first and third quartiles (n = 3 independent experiments). *$p < 0.05$, **$p < 0.01$. One-way ANOVA followed by Tukey's test for multiple comparisons. (F) SKW3 cells stably expressing clonal TCRs were cultured for 2 hr with varying numbers of untransduced HEK293T cells (HEK293T-UT) or HEK293T-BTNL3/8$^+$ cells. Representative contour plots from a single experiment display expression of CD3 and Nur77. (G) Expression of CD3 on unstimulated (black) or αCD3/αCD28-stimulated SKW3 cells (red) stably expressing the indicated TCRs. (H) Surface expression of CD3 and intracellular expression of Nur77 for the indicated SKW transductants cultured with HEK293T-UT cells (untreated) or stimulated with αCD3/αCD28 beads.

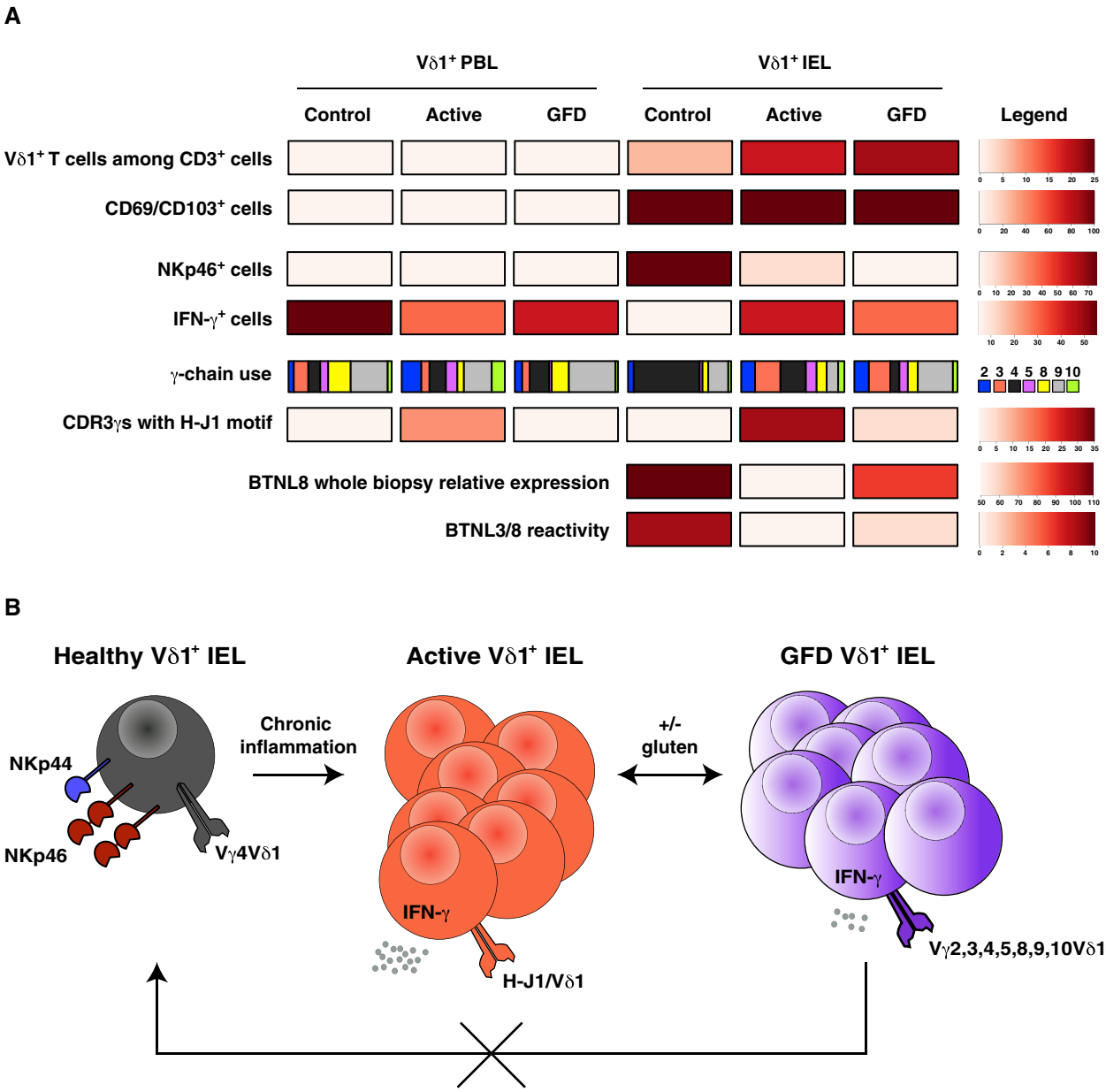

Figure S6. The Tissue-Resident Vδ1+ IEL Compartment Is Permanently Reshaped in CeD, Related to Figures 1–7

(A) Top: Vδ1+ IELs are expanded in patients with CeD and adopt a tissue-resident phenotype characterized by expression of CD69 and CD103. Mean frequency values are summarized by group/tissue. Middle/top: Vδ1+ IELs expressing NKp46 are lost in CeD and replaced by IFN-γ-producing Vδ1+ IELs. Mean frequency values are summarized by group/tissue. Middle/bottom: Vδ1+ IELs lose the *TRGV4* gene-associated 'gut signature' in patients with CeD (data summarized by group/tissue). This loss is associated with the emergence of CDR3γ sequences incorporating the H-J1 motif among Vδ1+ IELs in patients with active CeD. These H-J1+ CDR3γ sequences become less common after exclusion of dietary gluten. Bottom: *BTNL8* expression is lost in patients with active CeD, and Vδ1+ IELs no longer recognize BTNL3/8. Although *BTNL8* expression levels recover on a strict GFD, BTNL3/8 reactivity is permanently lost among Vδ1+ IELs. (B) Vδ1+ IELs in the healthy state (black) express NKp46 and NKp44, as well as Vγ4+/Vδ1+ TCRs that recognize BTNL3/8. These activating NCRs allow healthy Vδ1+ IELs to recognize and eliminate stressed, infected, or malignant IECs. In patients with CeD, decreased expression of *BTNL3 and BTNL8* is accompanied by a loss of Vγ4+/Vδ1+ IELs, which are replaced by Vδ1+ IELs (red) that produce IFN-γ in a gluten-dependent manner and express TCRγ chains enriched for the H-J1+ CDR3γ motif that fail to recognize BTNL3/8. These H-J1+ Vδ1+ IELs contract after withdrawal of dietary gluten, but are not replaced by NCR+ Vγ4+/Vδ1+ IELs. Instead, Vδ1+ IELs in patients with GFD-treated CeD are enriched for TCRs that fail to recognize BTNL3/8. Repertoire diversity also increases (purple color gradient), suggesting of a lack of selection pressure in the absence of gluten-induced inflammation. This model is consistent with a fundamental reshaping of the tissue-resident Vδ1+ IEL compartment after the onset of CeD.

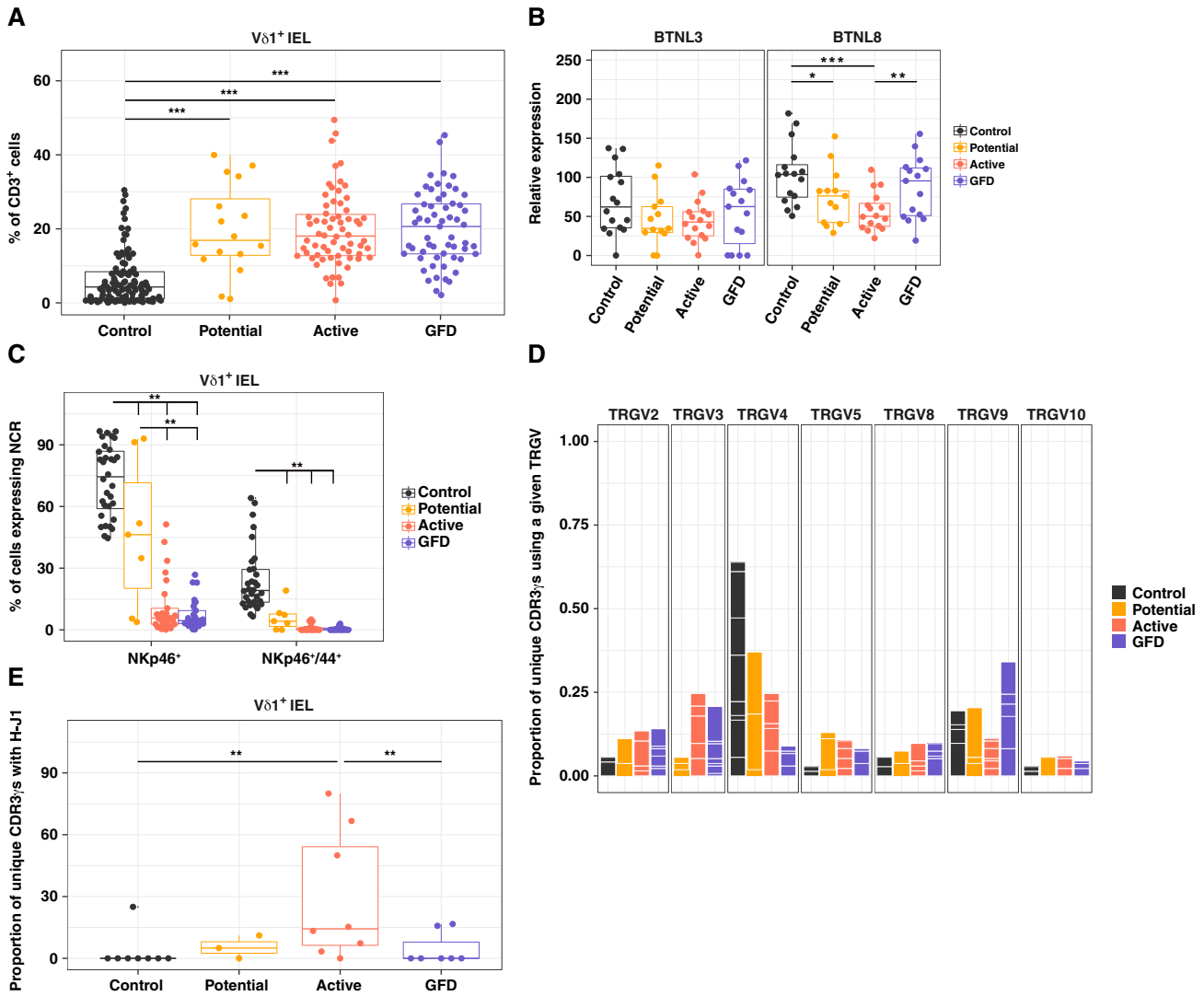

Figure S7. Alterations to the Vδ1$^+$ IEL Compartment Precede Tissue Damage in CeD, Related to Figure 7

(A) Frequency of Vδ1$^+$ cells among CD3$^+$ lymphocytes. Boxplot displays first and third quartiles. ***p < 0.001. One-way ANOVA with Tukey's test for multiple comparisons. (B) Expression of *BTNL3* and *BTNL8* relative to *GAPDH* in small intestinal biopsies determined via qPCR. Boxplots display first and third quartiles. *p < 0.05, **p < 0.01, ***p < 0.001. Kruskal-Wallis rank sum test with Dunn's test for multiple comparisons. (C) Frequency of Vδ1$^+$ IELs expressing NKp46 with or without NKp44. Boxplot displays first and third quartiles. **p < 0.01. One-way ANOVA with Tukey's test for multiple comparisons. (D) Proportion of unique CDR3γ sequences using a particular *TRGV* gene among Vδ1$^+$ IELs. White lines demarcate individual contributions. (E) Frequency of unique CDR3γ sequences incorporating the H-J1 motif among Vδ1$^+$ IELs. Boxplot displays first and third quartiles. **p < 0.01. Kruskal-Wallis rank sum test with Dunn's test for multiple comparisons.